FOR THE RECORD

Structure of a novel c_7-type three-heme cytochrome domain from a multidomain cytochrome *c* polymer

P. RAJ POKKULURI,[1,4] YURI Y. LONDER,[1,4] NORMA E.C. DUKE,[1] JILL ERICKSON,[1] MIGUEL PESSANHA,[2] CARLOS A. SALGUEIRO,[2,3] AND MARIANNE SCHIFFER[1]

[1]Biosciences Division, Argonne National Laboratory, Argonne, Illinois 60439, USA
[2]Instituto de Tecnologia Química e Biológica, Universidade Nova de Lisboa, Rua da Quinta Grande 6, 2780-156 Oeiras, Portugal
[3]Departamento de Química da Faculdade de Ciências e Tecnologia da Universidade Nova de Lisboa, Quinta da Torre, 2825-114 Caparica, Portugal

(RECEIVED January 12, 2004; FINAL REVISION February 27, 2004; ACCEPTED March 1, 2004)

Abstract

The structure of a novel c_7-type cytochrome domain that has two bis-histidine coordinated hemes and one heme with histidine, methionine coordination (where the sixth ligand is a methionine residue) was determined at 1.7 Å resolution. This domain is a representative of domains that form three polymers encoded by the *Geobacter sulfurreducens* genome. Two of these polymers consist of four and one protein of nine c_7-type domains with a total of 12 and 27 hemes, respectively. Four individual domains (termed A, B, C, and D) from one such multiheme cytochrome *c* (ORF03300) were cloned and expressed in *Escherichia coli*. The domain C produced diffraction quality crystals from 2.4 M sodium malonate (pH 7). The structure was solved by MAD method and refined to an *R*-factor of 19.5% and *R*-free of 21.8%. Unlike the two c_7 molecules with known structures, one from *G. sulfurreducens* (PpcA) and one from *Desulfuromonas acetoxidans* where all three hemes are bis-histidine coordinated, this domain contains a heme which is coordinated by a methionine and a histidine residue. As a result, the corresponding heme could have a higher potential than the other two hemes. The apparent midpoint reduction potential, E_{app}, of domain C is −105 mV, 50 mV higher than that of PpcA.

Keywords: multiheme cytochrome *c*; cytochrome c_7; *Geobacter metallireducens*; *Geobacter sulfurreducens*; heme coordination in *c*-type cytochromes; protein structure

c-Type cytochromes have hemes covalently bound to the protein through two thioether bonds with cysteine residues; the largest family consist of the class I molecules (Mathews 1985; Degtyarenko et al. 1997 [http://metallo.scripps.edu/PROMISE/]), where the fifth and sixth ligands of the hemes are histidine and methionine residues, respectively. Bis-histidine coordination is found in multiheme cytochromes (Degtyarenko et al. 1997 [http://metallo.scripps.edu/PROMISE/]): for example, class III (Coutinho and Xavier 1994), and class IV cytochromes (Deisenhofer et al. 1995), and in cytochrome *c* nitrite reductase (Einsle et al. 2000), and other four heme cytochromes (Leys et al. 2002). Only in class IV, the photosynthetic reaction center cytochrome *c* subunit, hemes of both coordination types are found in the same domain (Deisenhofer et al. 1995). Cytochrome *c* peroxidase has both a bis-histidine coordinated heme and a heme with His–Met coordination; however, these hemes are in separate domains (Fülöp et al. 1995; Shimizu et al. 2001). In general, hemes with His–Met coordination are expected to have more positive reduction potentials than hemes with His–His coordination (for review, see Dolla et al. 1994).

Reprint requests to: Marianne Schiffer, Biosciences Division, Argonne National Laboratory, Argonne, IL 60439, USA; e-mail: mschiffer@anl.gov; fax: (630) 252-3387.

[4]These authors contributed equally to this work.

Abbreviations: E_{app}, apparent midpoint reduction potential; MAD, multiple wavelength anamolous dispersion; PDB, Protein Data Bank.

Article published online ahead of print. Article and publication are at http://www.proteinscience.org/cgi/doi/10.1110/ps.04626204.

Among the multiheme cytochromes from the class III cytochrome family, the cytochromes c_3 from the sulfur- and sulfate-reducing bacteria are best studied (for review, see Mathews 1985; Coutinho and Xavier 1994; Aragao et al. 2003). They consist of about 120 amino acid residues and four covalently linked heme groups. The hemes are numbered sequentially according to the cysteine residues to which they are attached in the amino acid sequence. Heme IV is suggested to interact with hydrogenases (Aubert et al. 1997; Brugna et al. 1998). Although the sequence identity among the four-heme proteins is relatively low, ~25%, the positions and orientations of the hemes in the three-dimensional structures are maintained (Aragao et al. 2003). The three-heme cytochromes c_7 from Fe(III)-reducing bacteria (Seeliger et al. 1998; Afkar and Fukumori 1999; Lloyd et al. 2003) are structurally homologous to the four-heme cytochromes c_3, but are missing heme II of the cytochrome c_3 molecules and the amino acid chain segment that keeps that heme in place. For comparison with the more extensively studied four-heme cytochromes, the cytochrome c_3 nomenclature for labeling the hemes in the cytochrome c_7 proteins is maintained.

We have previously expressed in *Escherichia coli* and determined the structure of cytochrome c_7 from *Geobacter sulfurreducens*, designated PpcA, a protein with 71 residues that contains three covalently bound hemes (Londer et al. 2002; Lloyd et al. 2003; Pokkuluri et al. 2004). It is one of the smallest cytochrome *c*-type molecules with the highest ratio of hemes to protein residues. Searching the *G. sulfurreducens* genome with the PpcA sequence we identified three ORFs coding for proteins that are polymers formed with repeats of homologous c_7-type domains. Two of the proteins (coded by ORF00991 and ORF03300) have four repeats (total of 12 hemes) and one (coded by ORF03649) has nine repeats (total of 27 hemes) of the cytochrome c_7-type domain (Pokkuluri et al. 2004). We also found homologous polymers in the *G. metallireducens* genome (four unit polymers are encoded by Gmet_6, Gmet_8 and the nine unit polymer is encoded by Gmet_2 in the *G. metallireducens* genome [http://www.ncbi.nlm.nih.gov, accession number NZ_AAAS00000000]) with 77%, 75%, and 72% identity, respectively, with the ones identified in the *G. sulfurreducens* genome. We predicted based on the crystal packing observed in the PpcA crystals that the domains in the above polymers will be linearly arranged (Pokkuluri et al. 2004). The functions of the polymers are presently unknown. The repeats within each of the three poly-cytochrome c_7-type proteins are highly homologous. The repeat lengths are longer than that of the cytochrome c_7 PpcA molecule (71 residues); they vary from 73 to 82 residues.

These proteins appear to represent a new type of cytochrome. Interestingly, in each repeat of the multi-cytochrome c_7 sequences, the sixth His ligand to heme IV is absent, the homologous residue in the sequence is mostly Lys or Gln. We proposed earlier that either the Lys or Gln residues or one of the two conserved Met residues in the vicinity could be the second axial ligand to heme IV in those domains (Pokkuluri et al. 2004). Because the chain segments between the heme I and heme III binding sites are longer in the poly-cytochrome c_7-type domains than in the cytochrome c_7 molecule PpcA, the structure of this segment, and therefore the residue that forms the sixth ligand of heme IV, could not be predicted with confidence.

To characterize these cytochrome c_7-type domains, we have expressed in *E. coli* the four individual domains of the mature protein coded by ORF003300 (Fig. 1) of the *G. sulfurreducens* genome, and have determined the three-dimensional structure by X-ray diffraction of single crystals at 1.7 Å resolution of the third domain, domain C. In this manuscript, we describe the structural features of this protein in comparison with the structure of cytochrome c_7 (PpcA) from *G. sulfurreducens*. The alignment of the amino acid sequence of domain C with that of PpcA is shown in Figure 2.

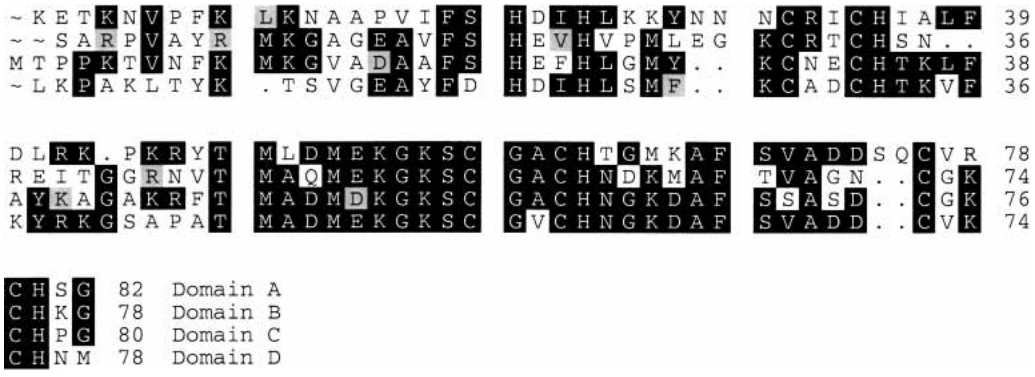

Figure 1. Sequence of ORF03300 from *G. sulfurreducens*; its four domains are aligned with each other.

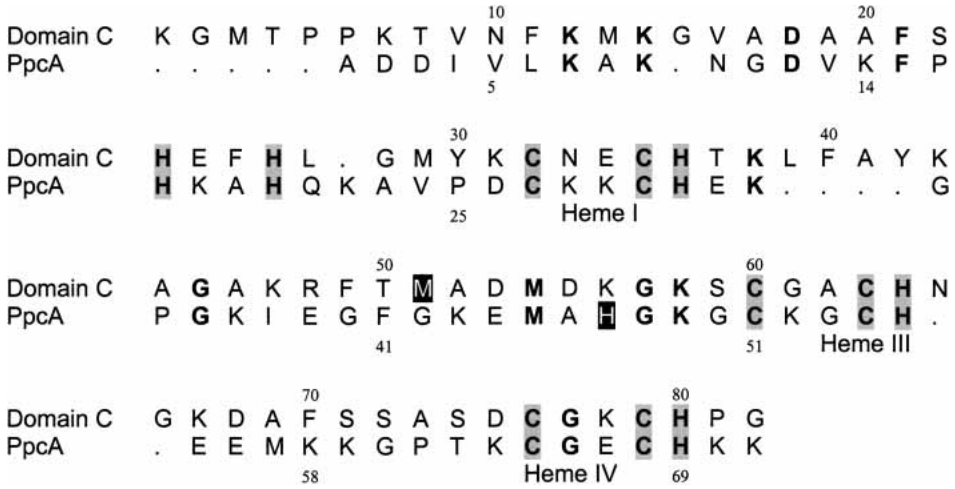

Figure 2. Amino acid sequence alignment of domain C of the four domain poly-c_7-type cytochrome (ORF03300) and cytochrome c_7 (PpcA) from *G. sulfurreducens*. Identical residues are shown in bold; the heme binding residues are shown in gray boxes and the heme numbering is indicated *below*. The sixth axial ligand to heme IV in both proteins is shown in a black box (note that these residues do not align in the sequence).

Results and Discussion

Cloning and expression of the domains

For cloning the single domains, the expression system described by Londer et al. (2002) was modified as follows: (1) Genes were cloned without adding extra N-terminal residues to their mature sequences; (2) the gene coding for periplasmic chaperone, Skp, known to facilitate folding of various proteins in the periplasm (Bothmann and Pluckthun 1998; Schäfer et al. 1999; Mavrangelos et al. 2001) was cloned immediately after the ampicillin-resistance gene to be expressed constitutively. The new vector is named pVA203 (its detailed description will be published elsewhere).

We cloned separately each of the four cytochrome c_7-type domains (A, B, C, and D) of the four-unit polymer (ORF03300) into the periplasmic expression vector pVA203. Domain A was cloned both as a fusion to the OmpA leader sequence and with its native leader sequence. All five constructs produced *c*-type cytochromes as judged by the pink color of the harvested cells. The overall yields of domains increased in the following order: A with native leader sequence << A with OmpA leader sequence < B < C << D. The yield of domain A was very low, and its isolation was not attempted. Domains B, C, and D were purified by cation-exchange chromatography and gel filtration as described previously (Londer et al. 2002). The yields of pure proteins per liter of cell culture were: domain B, 0.2 mg; domain C, 0.25 mg; domain D, 1.1 mg.

Structure determination

Crystals were obtained from domains C and D; crystals of domain C diffracted well and allowed structure determination at a resolution of 1.7 Å. The structure was solved by multiple wavelength anomalous dispersion (MAD) method with program CNS (Brünger et al. 1998) using data collected at the Fe K-absoption edge at the SBC beam line 19BM (APS). The structure was refined to 1.7 Å resolution with data collected at beam line 19ID (APS); the *R*-factor and *R*-free are 19.5% and 21.8%, respectively (see Table 1).

Comparison of domain C and PpcA

The structure of domain C clearly shows that the sixth ligand of heme IV is a methionine; we could not determine the identity of the coordinating residue based on the amino acid sequence alone. Domain C contains 82 amino acids, while PpcA has 71 amino acids. Although domain C also contains three hemes and similar number of amino acid residues its structure is different from that of the PpcA determined earlier in our laboratory (Figs. 3,4). Domain C, as cloned, has five additional residues at the N terminus compared to PpcA. The sequence alignment of the domains of ORF03300 shown in Figure 1 suggested that the N-terminal Lys and Gly residues of the cloned domain C should be at the end of domain B; however, they were included at the begining of domain C for proper periplasmic cleavage. Twenty-one out of 82 residues are identical between domain C and PpcA (Fig. 2), but only 16 residues have the same role in the protein structure; 11 of these residues bind the hemes. There is one deletion in domain C compared to PpcA; the equivalent residue of Lys 22 or Ala23 in PpcA is not present in domain C. There is an insertion of a Gly residue in the tip of the β-bend of domain C; four hydrophobic amino acids, Leu, Phe, Ala, and Tyr are inserted after the conserved lysine, Lys33 in PpcA; there is also an insertion of two residues (Asn and Gly) after the His residue of the heme III binding site.

Table 1. *Summary of data collection and crystallographic parameters*

Crystal parameters
Unit cell (Å) $a = b = 43.8$, $c = 123.8$
Space group $P4_12_12$

	MAD data				
	Inflection	Peak	High remote	Low remote (reference)	High res
Data collection					
Wavelength (Å)	1.74044	1.73769	1.69031	1.78780	1.03320
Resolution range (Å)	99.0–2.20	99.0–2.15	99.0–2.05	99.0–2.20	99.0–1.7
No. of unique reflections	6628	7072	8024	6594	13,958
Redundancy (last shell)	9.5 (3.4)	9.3 (3.5)	9.0 (2.6)	9.2 (3.4)	10 (11)
Completeness (last shell), %	99 (87)	99 (89)	97 (77)	98 (88)	99 (100)
Average I/σ (l) (last shell)	28 (2.6)	56 (9.4)	45 (4.2)	64 (9.2)	61 (13)
R-merge (last shell), %	8.7 (34)	6.8 (15.2)	6.8 (24.2)	4.1 (14.7)	5.0 (27.4)

	Inflection		Peak		Remote		All
Resolution range (50–2.4 Å)	Fried	Iso	Fried	Iso	Fried	Iso	
Phasing							
Phasing power	1.71	1.57	2.21	1.86	2.40	2.00	
FOM	0.45	0.44	0.46	0.44	0.37	0.36	0.81
Density modification, FOM							0.95

Refinement	
Resolution Range (Å)	99.0–1.7
σ cut-off used in refinement	0.0
No. of reflections	24,246
No. of nonhydrogen atoms refined (Average B-factor, Å^2)	
Protein	589 (24.6)
Heme	129 (19.0)
Water	105 (38.1)
R-factor, *R*-free[a] (all data)	0.195, 0.218
RMSD from ideal geometry	
Bond length (Å)	0.008
Angle (°)	3.6

[a] The test set for *R*-free calculation was comprised of 10% of the total reflections selected at random and were not used in refinement.

As was observed in the PpcA structure, domain C also has a two-stranded β-sheet segment near its N terminus, and five helical regions, one less than PpcA. The helical segments include the three heme-binding sites, the segment that contain the sixth ligands to hemes I, III, and the segment that contains the sixth ligand to heme IV. Although the latter segments in the two structures are in homologous positions in the amino acid sequences (Fig. 2), their relative positioning in structures compared to heme IV are different. In the case of PpcA, His47, the sixth ligand to heme IV is located at the end of the helical segment, whereas Met51, which is the sixth ligand to heme IV in domain C, is at the beginning of the helical segment. The rotamer conformation of the Met51 is chi1 −66, chi2 −50, chi3 −49. Lovell et al. (2000) found that this rotamer is the most observed in their data base; it is also one of the most observed for methionines in helical regions. Interestingly, this rotamer is not used by any of the methionines that are ligands to hemes in other cytochrome *c* proteins (P.R. Pokkuluri and M. Schiffer, unpubl.).

Domain C has a more conventional structure than PpcA. The number of hydrophobic residues larger than Ala in the core of domain C and the number of side-chain-to-main-chain hydrogen bonds (see Table 2) are more similar to what is observed for globular proteins in general; they are very low in PpcA. Domain C has 12 Lys and one Arg residue, compared with 17 Lys and no Arg residues in PpcA.

The ND1 atoms of all five of the histidine residues are hydrogen bonded to main-chain carbonyl oxygen atoms. Due to the differences in the structures, only two histidine ND1 atoms, from His 22 and His80, are hydrogen bonded to equivalent carbonyls in PpcA. In contrast to PpcA, none of the histidine residues in domain C are accessible to solvent.

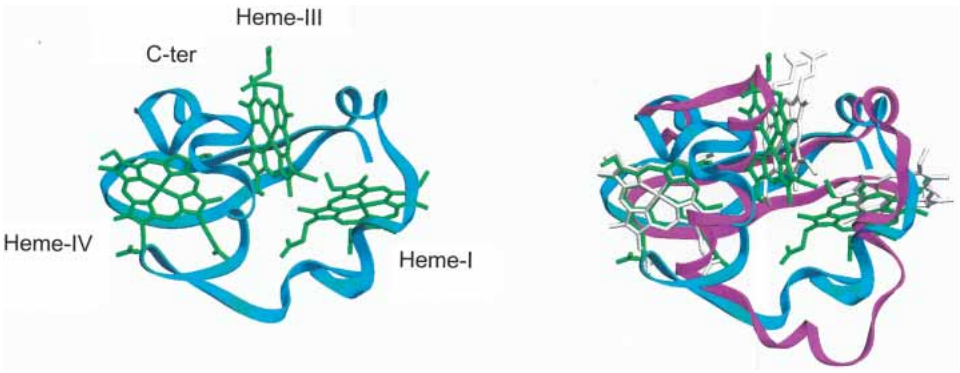

Figure 3. Ribbon drawing of domain C (*left*) and overlap of domain C and PpcA (*right*). Domain C and PpcA were overlapped using heme IV atoms. Domain C, blue; PpcA, magenta; hemes in domain C, green; hemes in PpcA, gray.

There is an unusual *cis*-peptide bond between His36 and Thr37 (Fig. 5). Nonproline *cis*-peptide bonds are very rare; they represent only 0.03% of the peptide bonds in PDB (Jabs et al. 1999). The conformation of the chain segment that consists of hydrophobic residues Leu39, Phe40, Ala41, and Tyr42 is probably made possible by the presence of the above *cis*-peptide bond in domain C. These residues shield heme I, the least exposed heme in this structure, from solvent. The ring of Phe40 is close to heme I; carbonyls of residues Phe40 and Ala41 are hydrogen bonded to the ND1 atom of His36, the fifth ligand to heme I. The ring of Tyr42 is near and close to parallel to His36.

All but one of the heme propionic acids form hydrogen bonds with a backbone amide nitrogen; in addition, a salt bridge is formed between Arg48 and propionic acid D of heme III. Heme III has the largest accessible surface area of 173 $Å^2$, followed by heme IV of 167 $Å^2$, and heme I is least exposed with 79 $Å^2$. In PpcA, heme I had the largest ac-

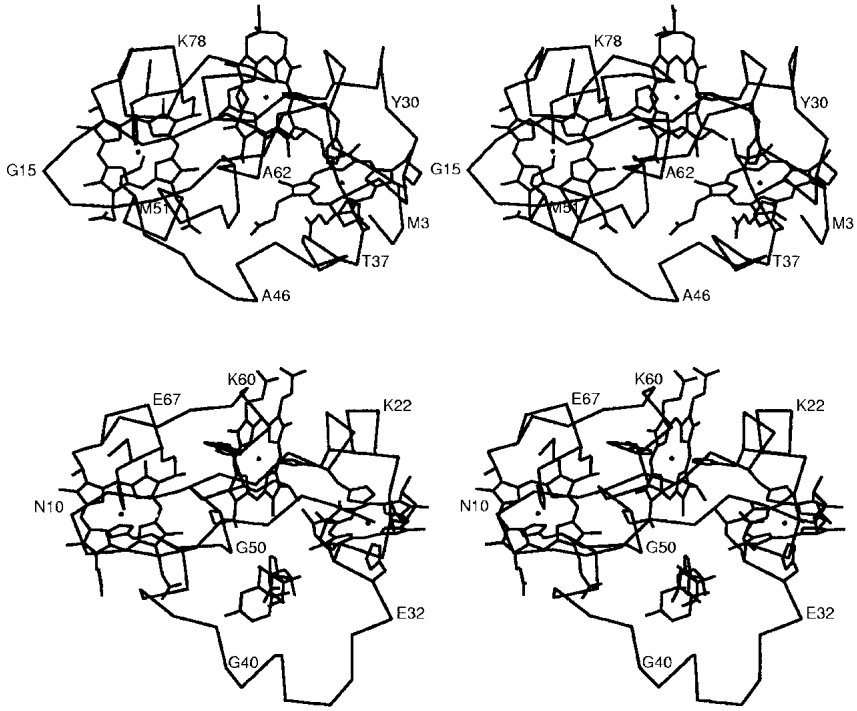

Figure 4. Stereo views showing hemes, α carbons, and side chains that bind the hemes in (*top*) domain C, (*bottom*) cytochrome c_7 (PpcA) from *G. sulfurreducens*. The PpcA structure shown also includes a molecule of deoxycholic acid in the *lower* part of the figure. Heme I is on the *right*, heme III is in the *middle*, and heme IV is located on the *left* side of the figures. The orientations of the hemes IV are the same in the two molecules. Note that the methionine residue that coordinates heme IV in domain C is in the *left* side of the figure.

Table 2. *Hydrogen bonds formed by heme propionic acid groups and by His residues*

Hydrogen bonded atoms		Distance (Å)
Heme I O2A	Ala44 N	2.85
Heme I O1D	Gly45 N	2.93
Heme III O2D	Phe70 N	2.93
Heme III O2D	Arg48 NH1	2.61
Heme IV O2A	Met51 N	2.76
Heme IV O1D	Phe49 N	2.88
His23 ND1	Pro6 O	2.75
His26 ND1	Ser22 O	2.87
His36 ND1	Phe40 O	2.89
His36 ND1	Ala41 O	3.16
His64 ND1	Phe70 O	2.90
His80 ND1	Ala17 O	2.78

cessible surface area of 225 $Å^2$ and heme III had the smallest one of 144 $Å^2$. In the full-length protein, we predict that only heme III would be exposed to the solution, whereas both hemes I and IV would be largely buried in the interface of neighboring domains. This is expected, as we predict that the four domains coded by ORF03300 will be linearly arranged in the full-length protein.

The iron to iron distances of the hemes III and IV, hemes III and I, and hemes IV and I, respectively, are 11.4, 12.0, and 17.8 Å in domain C compared to 11.2, 12.6, and 20.8 Å in PpcA. These Fe–Fe distances are probably determined by the differences in number of residues between the heme binding sites. Surprisingly, the iron to iron distances found in this c_7-type domain are closer to the ones observed in cytochromes c_3 (average Fe–Fe distances between hemes III and IV, hemes III and I, and hemes I and IV for six proteins are 11.1, 12.2, and 17.7 Å (Higuchi et al. 1984; Matias et al. 1993, 1996; Czjzek et al. 1994; Morais et al. 1995; Einsle et al. 2001).

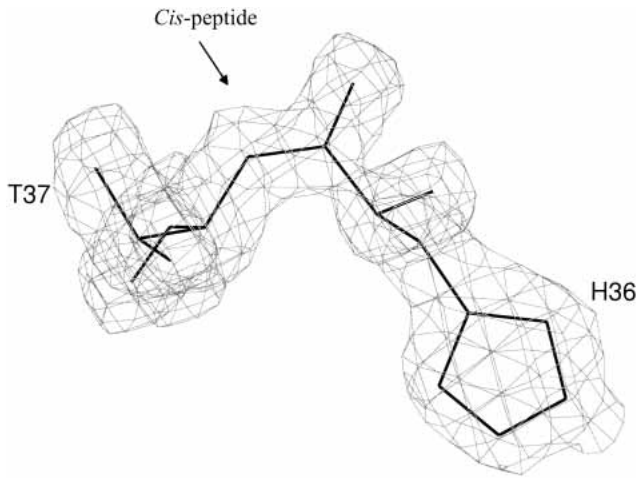

Figure 5. The *cis*-peptide bond observed in domain C between residues His-36 and Thr-37. Electron density in the final simulated-annealing composite omit-map generated by the program CNS is contoured at 1σ.

Crystal packing

As we previously observed in the PpcA crystal packing, the domain C molecules also form a long chain in the crystal. In domain C crystal, molecules are arranged in infinite chains parallel to the crystallographic *c* axis with the neighboring molecules related by a 4_1 axis (90° rotation and 1/4 unit cell translation) instead of one unit-cell translations along *a* and *b* axes as in the PpcA crystal (Pokkuluri et al 2004). In both crystals, the molecules in these chains are arranged such a way that heme I from one molecule is close to heme IV of the neighboring molecule. The iron to iron distance between these hemes in neighboring molecules in domain C is 13.8 Å compared to 12.9 Å in PpcA, but due to the difference in the relative angles of the prophyrin rings the heme edges are closer together in domain C crystals with the CMB atoms of heme I and heme IV 3.9 Å apart compared to 5.6 Å between the same atoms in PpcA crystals. Although the molecules also form infinite chains in the crystal of domain C, the N- and C-terminii cannot be connected, as they point in the opposite directions, and therefore, the crystal packing in domain C cannot form a model for the polymers, whereas the crystal packing in PpcA clearly suggested a model for them.

Visible redox titrations

The redox behavior of domain C and PpcA was investigated by redox titrations followed by visible spectroscopy. Results are given in Figure 6. The analysis of the redox titrations of the two proteins showed that the curve corresponding to domain C is clearly shifted to more positive reduction potential values relative to that of PpcA. This shift is reflected in the apparent midpoint reduction potential, E_{app}, of each protein (i.e., the point at which the oxidized and reduced fractions are equal). The value of E_{app} for PpcA is −155 mV; it is increased by 50 mV to −105 mV for domain C. The observed positive direction of the shift in the redox curves was expected (Mus-Veteau et al. 1992; Dolla et al. 1994) on the basis of different heme IV axial coordination for PpcA (His–His) and domain C (His–Met).

In summary, we have determined the structure of domain C of the four domain protein coded by ORF03300 of *G. sulfurreducens*. The structure has shown that the sixth ligand to heme IV is a methionine. This could not have been predicted based on sequence homology to three-heme cytochromes c_7. There is a conserved methionine at equivalent position in the sequences of all polymers made up of c_7-type domains (like domain C) found in *G. sulfurreducens* (Pokkuluri et al 2004) and *G. metallireducens*, suggesting that the sixth ligand to heme IV in all domains is a methionine.

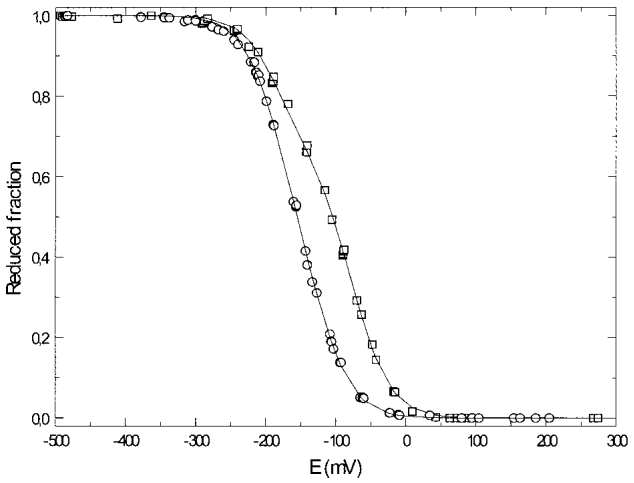

Figure 6. Visible redox titrations for domain C (open squares) and PpcA (open circles) at 298 K (pH 7.9). The molar fraction of the total reduced protein was fitted to the model described by Santos et al. (1984) and Wang et al. (1991), for various solution potentials. Solid lines indicate the results of the fits for the three macroscopic reduction potentials (vs. standard hydrogen electrode), which in domain C are −185 mV, −98 mV, and −52 mV, and in PpcA are −200 mV, −155 mV, and −110 mV.

These domains represent a new type of multiheme cytochrome *c* as they have two hemes with bis-His coordination and one with His–Met coordination. As expected, due to this difference in heme coordination, the apparent midpoint reduction potential of this domain is more positive compared to the cytochrome c_7 (PpcA).

Materials and methods

Cloning, expression, and purification of the domains

Cloning of the domains was carried out with modification of the methods previously described (Londer et al. 2002; Pokkuluri et al. 2004). A NotI restriction site was introduced at the end of the DNA fragment coding for the OmpA leader sequence of expression vector pCK32 (Londer et al. 2002). Mutagenesis resulted in Gln to Ala mutation in position "−2", a position that is considered nonessential for proper processing of a leader sequence during secretion (Nielsen et al. 1997). This modification allows cloning genes without adding extra N-terminal residues to their mature sequences. Further, a unique NcoI restriction site was created 8 bp downstream of the ampicillin resistance gene, and the gene coding for *E. coli* periplasmic chaperone, Skp, was cloned into this site. The new vector was named pVA203. DNA fragments coding for the putative domains were amplified from *G. sulfurreducens* genomic DNA and cloned into the vector pVA203. Domain A was cloned both as a fusion to the OmpA leader sequence and together with its native leader sequence. Compared to the alignment shown in Figure 1, one N-terminal residue was removed in domains B and D, and two preceding residues (Lys–Gly) were added to the N terminus of domain C to ensure proper cleavage of the modified OmpA leader sequence as predicted by the SignalP software (www.cbs.dtu.dk/services/SignalP; Nielsen et al. 1997).

Expression and purification of the domains were performed with slight modification of the procedure previously described (Londer et al. 2002); induction was carried out with 10 μM IPTG and a final gel-filtration step was added to the purification protocol.

Crystallization of domain C

The protein was crystallized by hanging drops from 2.4 M sodium malonate (pH 7) (Hampton Research, Index screen-27). Tetragonal crystals, space group $P4_12_12$ or $P4_32_12$, with a unit cell of $a = b = 43.8$ Å, $c = 123.8$ Å, diffracted to a resolution of about 1.7 Å at the Structural Biology Center's 19ID beam line at the Advanced Photon Source (APS).

Structure determination of domain C

Structure of domain C was determined by MAD method using four wavelength data sets (see Table 1) collected at the Fe K absorption edge at the 19BM (APS). Crystals were flash-cooled by briefly transferring them from mother liquor to a cryoprotectant solution (Index screen-27 containing 25% ethylene glycol). Data were processed with HKL2000 (Otwinowski and Minor 1997). Data collected at low-energy remote wavelength was used as the reference data set for structure determination using MAD method. Structure was solved with the program CNS (Brünger et al. 1998). After density modification the electron density map generated in space group $P4_12_12$ was of excellent quality (FOM = 0.95) and allowed model building. The protein model was built manually into the electron density map using the program CHAIN (Sack 1988) and refined against high resolution data collected at 19ID (APS). Refinement of the model was carried out with CNS (Brünger et al. 1998). There are no residues in the disallowed regions of the Ramachandran plot, and 87% residues are in most favored regions. The data collection and refinement parameters are summarized in Table 1. The structure and structure factors were deposited in the Protein Data Bank with accession code, 1rwj. Figure 3 was generated by the program SETOR (Evans 1993); Figures 4 and 5 were generated by the program CHAIN (Sack 1988). Accessible surface area was calculated by the program SURFACE (Lee and Richards 1971).

Sequence database search and analysis

Protein sequences homologous to the cytochrome c_7 were identified by searching the *G. sulfurreducens* and *G. metallireducens* genomes (www.ncbi.nlm.nih.gov, accession numbers NC_002939 and NZ_AAAS00000000) with the sequence of the cytochrome c_7 (PpcA, ORF01023) using BLAST software (Altschul et al. 1997). The SignalP software (http://www.cbs.dtu.dk/services/SignalP; Nielsen et al. 1997) was used for prediction of leader sequence cleavage sites. Genetic Computer Group Software package (Genetics Computer Group) was used for alignments.

Redox titrations followed by visible spectroscopy

Anaerobic redox titrations of domain C and PpcA, followed by visible spectroscopy were performed as described by Louro et al. (2001), with approximately 18 μM protein solutions in 100 mM Tris-maleate buffer at pH 7.9 and 298 ± 1 K. To check for hysteresis, each redox titration was performed in both oxidative and reductive directions, using sodium dithionite as the reductant, and potassium ferricyanide as the oxidant. To ensure a good equilib-

rium between the redox centers and the working electrode (Dutton 1978), a mixture of the following redox mediators were added to domain C and PpcA solutions, all at approximately 4 μM final concentration: Methylene Blue, gallocyanine, Indigo Tetrasulphonate, Indigo Trisulphonate, Indigo Disulphonate, anthraquinone-2,7-disulphonate, 2-hydroxy-1,4-naphthoquinone, anthraquinone-2-sulphonate, safranine O, diquat, benzylviologen, Neutral Red, methylviologen. For domain C the following additional mediators were also used, all at approximately 4 μM final concentration: *p*-benzoquinone, 1,2-naphtoquinone-4-sulfonic acid, 1,2-naphtoquinone, trimethylhydroquinone, phenasine methosulphate, and phenasine ethosulphate. The reduced fraction of each protein was determined using the α band peak, 552 nm for domain C and 551 nm for PpcA, according to the method described by Louro et al. (2001).

Acknowledgments

This work is supported by the U.S. Department of Energy's Office of Science, Biological and Environmental Research, Structural Biology, and NABIR programs under contract No. W-31-109-Eng-38. Use of the Argonne National Laboratory Structural Biology Center beam lines at the Advanced Photon Source was supported by the U.S. Department of Energy, Basic Energy Sciences, Office of Science, under contract No. W-310109-Eng-38. We thank Dr. Randy Alkire for help with data collection at the Fe K edge. Miguel Pessanha acknowledges Fundação para a Ciência e Tecnologia (FCT) for a doctoral fellowship (SFRH/5229/2001).

The publication costs of this article were defrayed in part by payment of page charges. This article must therefore be hereby marked "advertisement" in accordance with 18 USC section 1734 solely to indicate this fact.

References

Afkar, E. and Fukumori, Y. 1999. Purification and characterization of triheme cytochrome c7 from the metal-reducing bacterium, *Geobacter metallireducens*. *FEMS Microbiol. Lett.* **175:** 205–210.

Altschul, S.F., Madden, T.L., Schäffer, A.A., Zhang, J., Zhang, Z., Miller, W., and Lipman, D.J. 1997. Gapped BLAST and PSI-BLAST: A new generation of protein database search programs. *Nucleic Acids Res.* **25:** 3389–3402.

Aragao, D., Frazao, C., Sieker, L., Sheldrick, G.M., LeGall, J., and Carrondo, M.A. 2003. Structure of dimeric cytochrome *c*3 from *Desulfovibrio gigas* at 1.2 Å resolution. *Acta Crystallogr. D* **59:** 644–653.

Aubert, C., Leroy, G., Bruschi, M., Wall, J.D., and Dolla, A. 1997. A single mutation in the heme 4 environment of *Desulfovibrio desulfuricans* Norway cytochrome c_3 (Mr 26,000) greatly affects the molecule reactivity. *J. Biol. Chem.* **272:** 15128–15134.

Bothmann, H. and Pluckthun, A. 1998. Selection for a periplasmic factor improving phage display and functional periplasmic expression. *Nat. Biotechnol.* **16:** 376–380.

Brugna, M., Giudici-Orticoni, M.T., Spinelli, S., Brown, K., Tegoni, M., and Bruschi, M. 1998. Kinetics and interaction studies between cytochrome c_3 and Fe-only hydrogenase from *Desulfovibrio vulgaris* Hildenborough. *Proteins* **33:** 590–600.

Brünger, A.T., Adams, P.D., Clore, G.M., Delano, W.L., Gros, P., Grosse-Kunstleve, R.W., Jiang, J.-S., Kuszewski, J., Nigles, M., Pannu, N.S, et al. 1998. Crystallography and NMR system: A new software suite for macromolecular structure determination. *Acta Crystallogr. D* **54:** 905–921.

Coutinho, I.B. and Xavier, A.V. 1994. Tetraheme cytochromes. *Methods Enzymol.* **243:** 119–140.

Czjzek, M., Payan, F., Guerlesquin, F., Bruschi, M., and Haser, R. 1994. Crystal structure of cytochrome c_3 from *Desulfovibrio desulfuricans* Norway at 1·7 Å resolution. *J. Mol. Biol.* **243:** 653–667.

Degtyarenko, K.N., North, A.C.T., and Findlay, J.B.C. 1997. PROMISE: A new database of information on prosthetic centres and metal ions in protein active sites. *Protein Eng.* **10:**183–186.

Deisenhofer, J., Epp, O., Sinning, I., and Michel, H. 1995. Crystallographic refinement at 2.3 Å resolution and refined model of the photosynthetic reaction centre from *Rhodopseudomonas viridis*. *J. Mol. Biol.* **246:** 429–457.

Dolla, A., Blanchard, L., Guerlesquin, F., and Bruschi M. 1994. The protein moiety modulates the redox potential in cytochromes *c*. *Biochimie* **76:** 471–479.

Dutton, P.L. 1978. Redox potentiometry: Determination of mid-point potentials of oxidation-reduction components of biological electron-transfer systems. *Methods Enzymol.* **54:** 411–435.

Einsle, O., Stach, P., Messerschmidt A., Simon, J., Kröger, A., Huber, R., and Kroneck, P.M.H. 2000. Cytochrome *c* nitrite reductase from *Wolinella succinogenes*. *J. Biol. Chem.* **275:** 39608–39616.

Einsle, O., Foerster, S., Mann, K., Fritz, G., Messerschmidt, A., and Kroneck, P.M.H. 2001. Spectroscopic investigation and determination of reactivity and structure of the tetraheme cytochrome c_3 from *Desulfovibrio desulfuricans* Essex 6. *Eur. J. Biochem.* **268:** 3028–3035.

Evans, S.V. 1993. Hardware lighted three-dimensional solid model representations of macromolecules. *J. Mol. Graphics* **11:**134–138.

Fülöp, V., Ridout, C.J., Greenwood, C., and Hajdu, J. 1995. Crystal structure of the di-haem cytochrome *c* peroxidase from *Pseudomonas aeruginosa*. *Structure* **3:** 1225–1233.

Higuchi, Y., Kusunoki, M., Matsuura, Y., Yasuoka, N., and Kakudo, M. 1984. Refined structure of cytochrome c_3 at 1.8 Å resolution. *J. Mol. Biol.* **172:** 109–139.

Jabs, A., Weiss, M.S., and Hilgenfeld, R. 1999. Non-proline *cis* peptide bonds in proteins. *J. Mol. Biol.* **286:** 291–304.

Lee, B. and Richards, F.M. 1971. The interpretation of protein structures: Total volume, group volume distributions and packing density. *J. Mol. Biol.* **55:** 379–400.

Leys, D., Meyer, T.E., Tsapin, A.S., Nealson, K.H., Cusanovich, M.A., and Van Beeumen, J.J. 2002. Crystal structures at atomic resolution reveal the novel concept of "Electron-harvesting" as a role for the small tetraheme cytochrome *c*. *J. Biol. Chem.* **277:** 35703–35711.

Lloyd, J.R., Leang, C., Hodges Myerson, A.L., Coppi, M.V., Cuifo, S., Methe, B., Sandler, S.J., and Lovley, D.R. 2003. Biochemical and genetic characterization of PpcA, a periplasmic *c*-type cytochrome in *Geobacter sulfurreducens*. *Biochem. J.* **369:** 153–161.

Londer, Y.Y., Pokkuluri, P.R., Tiede, D.M., and Schiffer, M. 2002. Production and preliminary characterization of a recombinant triheme cytochrome c_7 from *Geobacter sulfurreducens* in *Escherichia coli*. *Biochim. Biophys. Acta* **1554:** 202–211.

Louro, R.O., Catarino, T., LeGall, J., Turner, D.L., and Xavier, A.V. 2001. Cooperativity between electrons and protons in a monomeric cytochrome c_3: The importance of mechano-chemical coupling for energy transduction. *Chembiochem.* **2:** 831–837.

Lovell, S.C., Word, J.M., Richardson, J.S., and Richardson, D.C. 2000. The penultimate rotamer library. *Proteins* **40:** 389–408.

Mathews, F.S. 1985. The structure, function and evolution of cytochromes. *Prog. Biophys. Mol. Biol.* **45:** 1–56.

Matias, P.M., Frazão, C., Morais, J., Coll, M., and Carrondo, M.A. 1993. Structure analysis of cytochrome c_3 from *Desulfovibrio vulgaris* Hildenborough at 1·9 Å resolution. *J. Mol. Biol.* **234:** 680–699.

Matias, P.M., Morais, J., Coelho, R., Carrondo, M.A., Wilson, K., Dauter, Z., and Sieker, L. 1996. Cytochrome c_3 from *Desulfovibrio gigas*: Crystal structure at 1.8 Å resolution and evidence for a specific calcium-binding site. *Protein Sci.* **5:** 1342–1354.

Mavrangelos, C., Thiel, M., Adamson, P.J., Millard, D.J., Nobbs, S., Zola, H., and Nicholson, I.C. 2001. Increased yield and activity of soluble single-chain antibody fragments by combining high-level expression and the Skp periplasmic chaperonin. *Protein Expr. Purif.* **23:** 289–295.

Morais, J., Palma, P.N., Frazão, C., Caldeira, J., LeGall, J., Moura, I., Moura, J.J.G., and Carrondo, M.A. 1995. Structure of the tetraheme cytochrome from *Desulfovibrio desulfuricans* ATCC 27774: X-ray diffraction and electron paramagnetic resonance studies. *Biochemistry* **34:** 12830–12841.

Mus-Veteau, I., Dolla, A., Guerlesquin, F., Payan, F., Czjzek, M., Haser, R., Bianco, P., Haladjian, J., Rapp-Giles, B.J., and Wall, J.D. 1992. Site-directed mutagenesis of tetraheme cytochrome c_3. Modification of oxidoreduction potentials after heme axial ligand replacement. *J. Biol. Chem.* **267:** 16851–16858.

Nielsen, H., Engelbrecht, J., Brunak, S., and von Heijne, G. 1997. Identification of prokaryotic and eukaryotic signal peptides and prediction of their cleavage sites. *Protein Eng.* **10:** 1–6.

Otwinowski, Z. and Minor, W. 1997. Processing of x-ray diffraction data collected in oscillation mode. *Methods Enzymol.* **276:** 307–326.

Pokkuluri, P.R., Londer, Y.Y., Duke, N.E.C., Long, W.C., and Schiffer, M.

2004. Family of cytochrome c_7-type proteins from *Geobacter sulfurreducens*: The structure of one cytochrome c_7 at 1.45 Å resolution. *Biochemistry* **43:** 849–859.

Sack, J.S. 1988. CHAIN—A crystallographic modeling program. *J. Mol. Graphics* **6:** 224–225.

Santos, H., Moura, J.J.G., Moura, I., LeGall, J., and Xavier, A.V. 1984. NMR studies of electron transfer mechanisms in a protein with interacting redox centres: *Desulfovibrio gigas* cytochrome c_3. *Eur. J. Biochem.* **141:** 283–296.

Schäfer, U., Beck, K., and Müller, M. 1999. Skp, a molecular chaperone of Gram-negative bacteria, is required for the formation of soluble periplasmic intermediates of outer membrane proteins. *J. Biol. Chem.* **274:** 24567–24574.

Seeliger, S., Cord-Ruwisch, R., and Schink, B. 1998. A periplasmic and extracellular *c*-type cytochrome of *Geobacter sulfurreducens* acts as a ferric iron reductase and as an electron carrier to other acceptors or to partner bacteria. *J. Bacteriol.* **180:** 3686–3691.

Shimizu, H., Schuller, D.J., Lanzilotta, W.N., Sundaramoorthy, M., Arciero, D.M., Hooper, A.B., and Poulos, T.L. 2001. Crystal structure of *Nitrosomonas europa* cytochrome *c* peroxidase and the structural basis for ligand switching in bacterial di-heme peroxidases. *Biochemistry* **40:** 13483–13490.

Wang, D.L., Stankovich, M.T., Eng, L.H., and Neujahr, H.Y. 1991. Redox properties of cytochrome c_3 from *Desulfovibrio desulfuricans* NCIMB 8372. Effects of electrode materials and sodium chloride. *J. Electroanal. Chem.* **318:** 291–307.